

# Classical optimisation of reduced density matrix estimations with classical shadows using N-representability conditions under shot noise considerations

Gian-Luca R. Anselmetti<sup>✉,\*</sup>, Matthias Degroote<sup>✉</sup>, Nikolaj Moll<sup>✉</sup>, Raffaele Santagati<sup>✉</sup>, and Michael Streif<sup>✉</sup>  
*Quantum Lab, Boehringer Ingelheim, 55218 Ingelheim am Rhein, Germany*  
 (Dated: November 28, 2024)

Classical shadow tomography has become a powerful tool in learning about quantum states prepared on a quantum computer. Recent works have used classical shadows to variationally enforce N-representability conditions on the 2-particle reduced density matrix. In this paper, we build upon previous research by choice of an improved estimator within classical shadow tomography and rephrasing the optimisation constraints, resulting in an overall enhancement in performance under comparable measurement shot budgets. We further explore the specific regimes where these methods outperform the unbiased estimator of the standalone classical shadow protocol and quantify the potential savings in numerical studies.

The simulation of quantum chemistry presents a hard challenge for the field of computation. In recent years, quantum computation has been proposed to aid quantum chemistry, offering to simulate complex systems that previously were out of reach for conventional methods [1–4]. However, current quantum computers are still limited in size and the number of operations due to noise and the absence of error correction [5]. As such, standalone quantum algorithms competing with the highly optimised methods of traditional quantum chemistry are still out of reach for the foreseeable future. This has opened up an avenue of research at the intersection of purely classical methods with the support of newly proposed simulation techniques on a quantum computer [6, 7].

Early efforts have sought to combine the strengths of classical and quantum algorithms in an approach labeled as hybrid quantum computation. In this spirit, recent work has tried to enhance some established classical methods with data gathered from shadow tomography, a powerful tool preparing efficient classical representations of quantum states prepared on a quantum computer for certain observables [8–11]. An example is the combination of this tool with traditional methods of quantum chemistry like Quantum Monte Carlo (QMC) [6] and Coupled Cluster (CC) [7], achieving improvement in accuracy in certain situations. These techniques are motivated by the fact that learning on quantum data in the form of classical shadows is known to provide quantum advantage [12] under certain conditions, identifying sampling on a quantum computer as a minimal-cost useful task.

While the aforementioned methods have focused on enhancing classical methods with quantum data, other work has sought to apply techniques developed in classical quantum chemistry to quantum computation, e.g., constraints stemming from the N-representability conditions (limiting the space of valid reduced density matrices (RDM) that can stem from a physical wavefunction) to enhance quantum readout [13–15]. The goal of these works is to optimise measurement methods in sampling

from an unknown quantum state, mostly trying to decrease sample variance and reduce sensitivity to device error [13, 14] and to decrease the shot budget of shadow tomography [15] with the use of v2rdm [16, 17], a method casting the N-representability conditions into a semidefinite program.

In this paper, we expand on recent work [15] by improving how to constrain the semidefinite program by using the entire 2-RDM estimate from a classical shadow. We also further explore the role of shot noise in estimation problems with and without the use of v2rdm in the classical shadow tomography. We establish regimes where the method can lead to savings in shot budgets of up to a factor of 15 over the non-optimised estimate. As for industrial relevancy, extracting ground state energies from this scheme does not lead to an application per se. The promise lies more in the efficient extraction of further chemically relevant observables like e.g., molecular forces for geometry optimisations or molecular dynamics [18, 19], as this is paramount to compete with established classical methods [20]. As fault-tolerant algorithms require a large overhead to extract expectation values of observables on ground states [21, 22], the main motivation was to see if sampling shadows of ground states from a quantum computer could help extract reduced density matrices more efficiently from a v2rdm procedure and whether it could be competitive to obtain expectation values when compared to these existing costly quantum algorithms.

The manuscript is structured the following way: First, we give a brief introduction to shadow tomography (Sec. I) and v2rdm (Sec. II). The former is focused on fermionic tomography respecting particle number and spin-preservation, and the latter briefly introduces core concepts of the constraints respected in our optimisation and how to deal with inequalities when casting semidefinite programs. We then describe the two additional constraints derived from quantum data (Sec. III), which we consider in our numerics, one from previous work [15] and one introduced in this work. We then simulate performance for various systems (Sec. IV) and compare it with the pure classical estimate and the pure quantum

\* gian-luca.anselmetti@boehringer-ingelheim.com

estimate derived from shadow tomography without re-optimising the 2-RDM to respect the N-representability conditions.

## I. CLASSICAL SHADOW PROTOCOL

Classical shadows, a scheme introduced in [8] based on the shadow tomography proposal [23], can predict many properties of a quantum system with a number of measurements which scale logarithmically with the number of properties measured. The task of the protocol is estimating the expectation value of multiple observables  $\langle O_i \rangle$  on unknown quantum state  $\rho$ . This requires the preparation of multiple copies of the state measured under random unitaries  $U$  drawn from an ensemble  $\mathcal{U}$ , resulting in the measurement outcome  $|b\rangle$ . Averaging over the results constitutes the measurement channel

$$\mathcal{M}(\rho) = \mathbb{E}_{U \sim \mathcal{U}} \left[ \sum_{b \in \{0,1\}^N} \langle b | U \rho U^\dagger | b \rangle U^\dagger | b \rangle \langle b | U \right]. \quad (1)$$

The collection of random unitaries  $U$  and associated measurement outcomes  $|b\rangle$  is referred to as a classical shadow. For each of these pairs, the measurement channel can be inverted to build an unbiased estimator of the quantum state

$$\hat{\rho} = \mathcal{M}^{-1} (U^\dagger |b\rangle \langle b| U). \quad (2)$$

From this classical estimator, one can infer the expected values of the desired observables  $\langle O_i \rangle = \text{Tr}(O_i \rho)$ . The quality of the inverse of the measurement channel  $\mathcal{M}^{-1}$  and the efficiency of the classical and quantum procedures depend on the chosen ensemble of unitaries and the associated observables one estimates from the quantum state.

Multiple choices for the ensembles and associated classical estimation schemes have been proposed [9–11]. We focus here on shadow estimation schemes twirling over the particle number restricted ensemble of matchgates [11]. This constitutes an efficient estimation scheme independent of the number of qubits,  $N$ , and its quantum cost scales only in the number of occupied fermionic modes  $\eta$ , which is the particle number of the trial state. This ensemble is usually referred to as the ensemble of single-particle basis rotations or orbital rotations  $U(u)$ , which define all valid transformations between different sets of the fermionic creation and annihilation operators  $a_q$  and  $a_q^\dagger$  by

$$U^\dagger(u) a_p^\dagger U(u) = \sum_{q=1}^N u_{pq} a_q^\dagger, \quad (3)$$

where  $u \in \mathbb{C}^{N \times N}$  is a unitary matrix defining the change of basis of the fermionic modes, with their representation  $U(u) \in \mathbb{C}^{2^N \times 2^N}$  in Hilbert space. We refer to

the submatrix restricted to the  $k$ -particle subspace as  $U_k \in \mathbb{C}^{\binom{N}{k} \times \binom{N}{k}}$ , and therefore  $U_{k=2}$  as the restriction to the two-particle subspace. We further restrict unitaries beyond preserving particle number to also preserve spin in Appendix C as these are the most important symmetries for molecular systems.

In general, expectation values of generic  $k$ -particle reduced density matrices ( $k$ -RDM) can be inferred from this procedure [11], we will only handle the two ( $k=2$ )-particle reduced density matrices as no higher order density matrices are required for the purpose of estimating the observables of our interest. Our task, therefore, is estimating the quantity:

$$\left\langle \frac{2}{S} \hat{\mathbf{D}}^{pqrs} \right\rangle = \text{Tr} [a_p^\dagger a_q^\dagger a_s a_r \rho], \quad (4)$$

for any quantum state  $\rho$ .  $\frac{2}{S} \hat{\mathbf{D}}^{pqrs}$  is the shadow estimator of the 2-RDM, and the subscript prefix  $S$  differentiates it from, e.g., the analytic 2-RDM  ${}^2\mathbf{D}^{pqrs}$  of a quantum state in the following.

The single-shot estimator for the expectation value of the 2-RDM for a measurement string  $b$  in the computational basis under the basis transformation generated by  $u$  is given by [11]

$$\frac{2}{S} \hat{\mathbf{D}}^{pqrs} = \left\langle r, s \left| U_{k=2}(v_b u) E_{\eta, k=2} U_{k=2}^\dagger(v_b u) \right| p, q \right\rangle, \quad (5)$$

where the basis states  $\langle r, s |$  and  $|p, q\rangle$  are defined by  $\langle r, s | = \langle 0 | a_s a_r$  and  $|p, q\rangle = a_p^\dagger a_q^\dagger |0\rangle$ , indexing elements of the reduced density matrix. The matrix  $v_b$  implements a rotation of  $b$  into the ordered string  $\{11 \dots 00\} = \{1^{\otimes \eta}\} + \{0^{\otimes (N-\eta)}\}$  and the operator  $E_{\eta, k}$  is defined as

$$E_{\eta, k=2} = \sum_{p, q \in \{1, \dots, N\}} |p, q\rangle \langle p, q| \frac{\binom{\eta - s'}{2 - s'} \binom{N - \eta + s'}{s'}}{(-1)^{2+s'} \binom{k}{s'}}. \quad (6)$$

with  $s'(p, q)$  being the number of shared indices with the reference determinant / Hartree Fock  $|p=1, q=1\rangle$ .

$$s'(p, q) = \begin{cases} 2 & p=1 \wedge q=1 \\ 1 & p=1 \vee q=1 \\ 0 & p \neq 1 \wedge q \neq 1 \end{cases}$$

The *average* shot variance of the 2-RDM estimator in Eq. 5 is then bounded by

$$\mathbb{E}_{pqrs} \left[ \text{Var} \left[ \left\langle \frac{2}{S} \hat{\mathbf{D}}^{pqrs} \right\rangle \right] \right] \leq \binom{\eta}{2} \left( 1 - \frac{\eta-2}{N} \right)^2 \left( \frac{1+N}{1+N-2} \right), \quad (7)$$

which scales as  $\mathcal{O}(\eta^2)$ . The estimator in Eq. (5) is only classically efficient for constant  $k$  [11], as is the case here for  $k=2$ .

## II. V2RDM

Variational methods using the 2-RDM as a more compact stand-in for the wavefunction, as it contains all the information to calculate the energy, molecular forces, dipole moments, etc., were developed at the beginning of the 1950s [24]. Originally obtaining energies that were too low [25], as unrestricted optimisation results in 2-RDMs not stemming from a physical wavefunction, were violating the variational principle. Once imbued with the concept of *N-representability* conditions, restricting the space of obtainable 1- and 2-RDMs in optimisation, conditions in an ever-increasing order were developed to guide variational methods to obtain physical results when traversing the space of 2-RDMs. Recent high-performance implementations using GPUs and CPUs of these methods have led to the capability to treat larger scale systems, e.g., 3,7-circumjacent in a (64e, 64o) active space [16]. A brief treatment of the theory behind the workings of the algorithm will follow, but there are further resources [16] for a more in-depth introduction to the topic.

In general, v2rdm is based on a convex optimisation in the form of a semidefinite program. The merit/cost function is formulated as a vector  $\mathbf{c}$ , containing the coefficients to score a solution vector  $\mathbf{x}$  over an inner product  $\mathbf{c}^T \mathbf{x}$  to be minimized. We use the energy under the Hamiltonian  $E [{}^2\mathbf{D}]$  as the cost function. The N-representability conditions are formulated as a system of linear equations, containing the set of linear equations embedded into the rows of a matrix  $\mathbf{A}$  and their respective solutions as a solution vector  $\mathbf{b}$ , while the entries of  $\mathbf{x}$  are cast into a block diagonal form in a matrix  $M(\mathbf{x})$ , where the matrix and therefore the individual blocks are to be kept positive semidefinite during optimisation. The full set of equations is summarized as

$$\begin{aligned} & \min_{\mathbf{x}} \mathbf{c}^T \mathbf{x} \\ & \text{such that } \mathbf{A}\mathbf{x} = \mathbf{b} \\ & \text{and } M(\mathbf{x}) \succeq 0. \end{aligned} \quad (8)$$

In our case, the individual elements of  $x$  are associated with the individual entries of the 1-RDM  ${}^1\mathbf{D}$  and 2-RDM  ${}^2\mathbf{D}$ , and further derived RDM-like quantities like the hole-particle 1-RDM  ${}^1\mathbf{Q}^{pq} = \langle \psi | a_p a_q^\dagger | \psi \rangle$  and similar quantities derived from the 2-RDM, that appear in more elaborate N-representability conditions [15]. These are often referred to as the Q- and G-conditions, which come at an increased computational cost but lead to higher precision in the end result. Further constraints using the 3-RDM entries have been developed but won't be covered here. The block diagonal structure defined by  $M(\mathbf{x})$  takes the form of

$$M(\mathbf{x}) = \begin{pmatrix} {}^1\mathbf{D} & 0 & 0 & 0 & 0 & 0 \\ 0 & {}^1\mathbf{Q} & 0 & 0 & 0 & 0 \\ 0 & 0 & {}^2\mathbf{D} & 0 & 0 & 0 \\ 0 & 0 & 0 & {}^2\mathbf{Q} & 0 & 0 \\ 0 & 0 & 0 & 0 & {}^2\mathbf{G} & 0 \\ 0 & 0 & 0 & 0 & 0 & \dots \end{pmatrix} \succeq 0 \quad (9)$$

As there is an exponential amount [26] of N-representability conditions, enforcing all of them is computationally unfeasible and one truncates the conditions usually at conditions of second or third order. At the second order, there are efficient algorithms in solving the resulting semidefinite program scaling as  $\mathcal{O}(N^4)$  in memory and  $\mathcal{O}(N^6)$  in compute, e.g. a boundary-point method *BDSDP* [27–29], and a matrix-factorisation based procedure *RRSDP* [30]. In total, the N-representability conditions usually considered in v2rdm can be summarized in the following way [15]

$$\min_{{}^2\mathbf{D}} E [{}^2\mathbf{D}] \quad (10)$$

$$\text{such that } {}^2\mathbf{D} \succeq 0 \quad (11)$$

$${}^2\mathbf{Q} \succeq 0 \quad (12)$$

$${}^2\mathbf{G} \succeq 0 \quad (13)$$

$$\text{Tr} ({}^2\mathbf{D}) = \eta(\eta - 1) \quad (14)$$

$${}^2\mathbf{Q} = f_Q ({}^2\mathbf{D}) \quad (15)$$

$${}^2\mathbf{G} = f_G ({}^2\mathbf{D}). \quad (16)$$

$f_G$  and  $f_Q$  are linear mappings between  ${}^2\mathbf{G}, {}^2\mathbf{Q}$  and  ${}^2\mathbf{D}$ . We use a spin-adapted v2rdm code and also enforce spin-adapted constraints from the classical shadow; for further details when adapting for spin, consult the Appendix A. To these traditional constraints, we add now additional constraints stemming from the classical shadow measurements on a quantum computer.

## III. SHADOW CONSTRAINTS

We consider two different sets of constraints stemming from the output of a quantum computer, further constraining the optimisation problem. The first way of constraining the optimisation problem, referred to as constraint (1) from here, is building an  $\epsilon$ -ball around all the elements of the true 2-RDM  ${}^2\mathbf{D}^{pqrs}$  from the estimator  ${}^2_S\hat{\mathbf{D}}^{pqrs}$  in Eq. 5 and estimating the radius of the ball  $\epsilon_1$  by means of the upper bounds of the variance from Eq. 7.

$${}^2_S\hat{\mathbf{D}}^{pqrs} - \epsilon_1 \leq {}^2\mathbf{D}^{pqrs} \leq {}^2_S\hat{\mathbf{D}}^{pqrs} + \epsilon_1 \quad (17)$$

This results in  $2N^4$  additional constraints to the optimisation, which are of constant size. These can further be divided into restrictions on each spin sector as

discussed in Appendix A. In general, the classical resources needed to calculate the estimator stemming from the classical shadow in Eq. 5 scale as  $\mathcal{O}(N^5)$  in the classical post-processing compared to the scaling  $\mathcal{O}(N^6)$  of the semidefinite program. The classical optimisation, therefore, adds a linear multiplicative overhead in classical computational cost while potentially reducing the number of quantum resources/shots required to reach a given precision. There exists a more efficient way of estimating from a classical shadow using Pfaffians [10, 11] not described here, which could bring this cost down even more.

The second constraint, referred to as constraint (2), introduced in [15] is based on the diagonal part of the 2-RDM, measured in the computational basis under  $m$  random single-particle rotations  $U_m$  from [11]

$$S_m^{pq} = \left\langle \Psi \left| \hat{U}_m^\dagger \hat{a}_p^\dagger \hat{a}_q^\dagger \hat{a}_q \hat{a}_p \hat{U}_m \right| \Psi \right\rangle. \quad (18)$$

This leads to  $2mN^2$  additional constraints, with  $N^2$  entries. The factor of 2 follows from constraining both sides of the inequality (see App. B for more details):

$$S_m^{pq} - \epsilon_2 \leq X_m^{pq} \leq S_m^{pq} + \epsilon_2, \quad (19)$$

with

$$X_m^{pq} = \left( (U_m \otimes U_m)^2 D (U_m \otimes U_m)^T \right)^{pq}, \quad (20)$$

where  $\epsilon_2$  marks the error on each element due to shot noise and device error. We only investigate behavior under shot noise considerations in this manuscript, but as device error can also be modeled under similar Gaussian perturbations to the correct RDM one could further study behavior under noisy conditions [13, 15].

#### IV. NUMERICS

In this section, we numerically investigate the performance of the proposed optimisation of the 2-RDM when using the two different constraints (Eq. 17 and Eq. 19, labeled (1) and (2)) stemming from the classical shadow estimation in comparison with the estimate stemming from a vanilla v2rdm estimation without any additional constraints and an estimate stemming from a classical shadow estimation without any v2rdm post-optimisation of the estimate (Eq. 5). To allow for comparison between the two constraints, their measurement shot budgets are considered in the following way: For more efficient numerical considerations, the estimate from a classical shadow for (1) is simulated by adding Gaussian noise to the 2-RDM from an FCI calculation where the strength of the perturbation on each element is calculated by the bound of the shot variance of each element from Eq. 7 converted into a standard deviation by dividing by the number of shots taken at the respective point.

Previous work [7, 31] has shown this to be an accurate noise model for the estimate of the classical shadow. As the constraint for (2) in Eq. 19 relies on measuring the diagonal elements of the 2-RDM under random basis rotations, we consider the average variance of one of these diagonal elements. For e.g. the  ${}^2D_{\alpha\beta}$  the expectation value of a diagonal element of the 2-RDM  $\mathbb{E}[S_{pq}]$  can be calculated by

$$\mathbb{E}[S^{pq}] = (N_\alpha N_\beta)^2 / \eta^2, \quad \text{Var}[S^{pq}] = 1 - \mathbb{E}(S^{pq})^2, \quad (21)$$

where  $N_\alpha, N_\beta$  are the number of  $\alpha, \beta$  electrons and  $\eta = N_\alpha + N_\beta$ . The respective variance  $\text{Var}[S_{pq}]$  follows from the observable mapping down to a Pauli observable ( $Z$ ) when measuring in the computational basis after the random basis transformation. To allow for equal shots for both ways of constraining the problem, the number of basis  $m$  sampled when constraining with Eq. 19 is taken to fulfill

$$\mathbb{E}_{pqrs} \left[ \text{Var} \left[ \left\langle \frac{2}{S} \hat{\mathbf{D}}^{pqrs} \right\rangle \right] \right] \approx m \text{Var}[S^{pq}] \quad (22)$$

rounded up to the closest integer  $m$ . As the bound of the shot variance given in Eq. 7 is also only bounding the *average* shot variance of an entry of the 2-RDM we deem this a fair comparison.

One way to view the two different constraints is as follows: measuring the diagonal elements, one *oversamples* measurements under the same basis rotation, so constraint (1) can be viewed as the limit of (2) when sampling in a new basis for every new shot and using the estimator in Eq. 5. As changing the basis requires reconfiguring the quantum circuit, this is usually associated with increased cost, and *oversampling* has been explored in Ref. [7] for potentially reducing cost in shadow estimation when accounting for this cost. We do not include this potentially increased cost here, but it can also be accounted for when constraining in (1) by increasing the bound of the variance from Eq. 7. Covariances are not considered here, as previous work has shown numerical evidence that no covariances are present when estimating orthogonal elements in classical shadow estimation using matchgates [7, 31].

Our implementation extends an open source version of a v2rdm code using libsdp, providing efficient solvers for the semidefinite program [16, 26] with the constraints mentioned above. We further use Openfermion [32] to build the correct Hilbert space representation of our basis rotations in the correct subspace to build our constraints and simulate measurements on a quantum computer.

We use our test systems,  $N_2$  in cc-pvdz basis in a (10,8) active space and benzene in the STO-3G in a (16,16) active space to investigate how system size affects the estimation. As previously mentioned, we are mostly concerned with improving the estimate of the 2-RDM from the shadow estimation scheme. Improvements in energy estimation we deem less interesting as one has access to more efficient ways of measuring the energy, e.g., double factorisation [33, 34] or tensorhypercontraction [35]. Constructing the Hilbert-Space

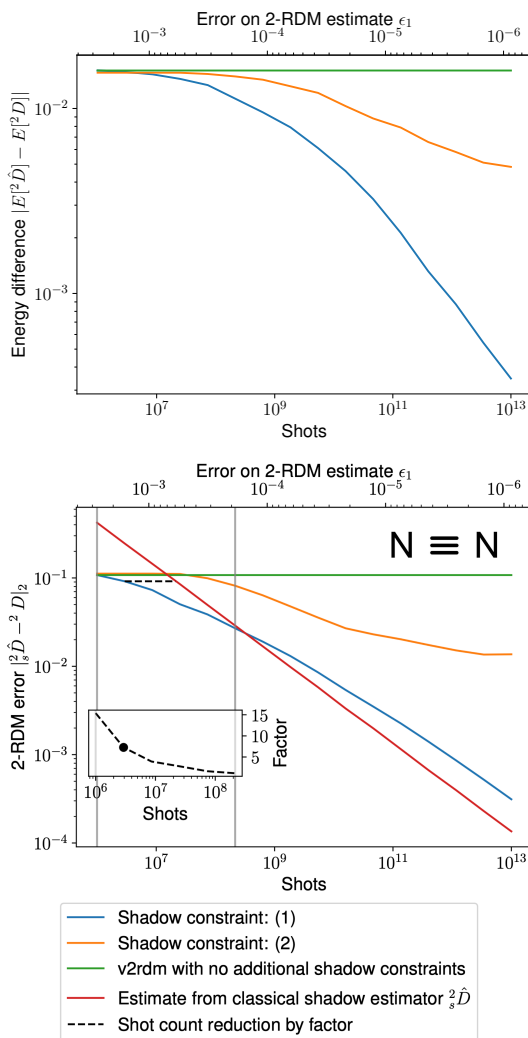


FIG. 1. Top: Energy error of the estimate of the ground state energy for  $N_2$  in dependence on the number of shots spent on the quantum shadow constraints included in the optimisation. Bottom: 2-RDM error in the Frobenius norm towards the true 2-RDM stemming from an FCI calculation of  $N_2$  in dependence on the number of shots spent on the quantum shadow constraints included in the optimisation. Inset quantifies the factor of improvement over the estimate coming just from the classical shadow at the same level of error (red). The dot in the inset corresponds to the dashed line in the outer figure as a guide to the eye and clarification.

unitaries needed for (2) becomes fairly costly at large system sizes, and consequently we only investigate constraint (1) for the largest of the test systems, benzene.

For the smaller active space (10,8) for  $N_2$ , looking at the energy, we find shadow constraint (1) outperforming shadow constraint (2) over the range of the shot interval investigated (Fig. 1, top). For the estimate of the 2-RDM compared to the true 2-RDM (Fig. 1, bottom) we also find shadow constraint (1) outperforming constraint (2) consistently. Above  $10^6$  shots, shadow constraint (1) improves over the plain v2rdm implementation, whereas

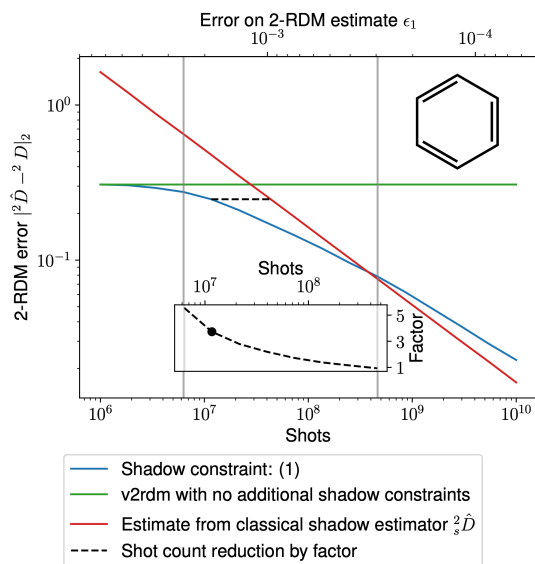


FIG. 2. 2-RDM error in the Frobenius norm towards the true 2-RDM stemming from an FCI calculation of benzene in a (16,16) active space in dependence of the number of shots spent on the quantum shadow constraints included in the optimisation. Inset quantifies the factor of improvement over the estimate coming just from the classical shadow at the same level of error (red). The dot in the inset corresponds to the dashed line in the outer figure as a guide to the eye and clarification.

the unadapted shadow estimation only improves above  $10^7$  over the purely classical estimate. Constraint (1) improves over the shadow estimate up until  $2 \times 10^8$  shots, where the shadow estimator overtakes the combined estimate, reaching a reduction of up to a factor of 15 required shots to reach the same precision. The threshold at  $2 \times 10^8$  can be explained by the energy acting as the cost function in optimisation: At some point, the optimiser biases the estimate by improving the entries of the 2-RDM with high weight from the Hamiltonian at the cost of the other entries, losing precision over the unbiased estimate of the classical shadow estimation performed on the true ground state. Shadow constraint (2) does not improve over v2rdm without constraints in the low shot regime or the estimate from classical shadow estimation at the  $10^7$  shots threshold.

For the large active space (16,16) for benzene (Fig. 2), we find a qualitatively very similar looking relationship between plain v2rdm, classical shadow estimation, and v2rdm with shadow constraint (1): At an error that corresponds roughly with  $10^{-3}$  the shadow estimation beats the purely classical estimate. v2rdm with shadow constraint (1) improves over both the other estimates for roughly two orders of magnitudes of shot budgets before the bias introduced into the estimate loses over the unbiased shadow estimation technique. Improvement factors also seem to be a bit lower in this scenario, only reaching up to a factor of 5.

## V. DISCUSSION

To conclude, our simulations show that v2rdm can help classical shadow estimation to increase precision for a given shot budget in certain regimes. We find up to a factor of 15 in improvement for  $N_2$ , although the factor of improvement is largest when being close to the result of the purely classical estimate. This improvement seems to be reduced for larger systems. For high precision estimates, the bias introduced seems to lose out over the unbiased estimate from shadow estimation. Nonetheless, when quantum resources are scarce in near- and mid-term shadow estimations trying to extract 2-RDM quantities from a state to extract, e.g., forces and other molecular properties beyond ground state energies, classically optimising the estimate from a classical shadow can lead to increased precision at a fixed quantum cost. Although the window where v2rdm actually improves the estimate is limited, for estimations where high precision is necessary, e.g., chemistry applications, this does not solve the

cost of extracting a 2-RDM from a quantum device. As we have investigated scaling of epsilon under the standard quantum limit  $\frac{1}{\epsilon^2}$ , the cost savings would become much more dramatic for recently proposed procedures [36] with better scaling in  $N$  at the cost of increased scaling in the error  $\epsilon$ .

As the optimisation under the energy as a cost function seems to introduce a bias limiting the applicability window where the combined methods improve over pure shadow estimation, changing the cost function to, e.g., the 1-norm of the 2-RDM [13, 15] might be an avenue in further improvement of the scheme presented here.

## VI. ACKNOWLEDGMENTS

We thank Nicholas Rubin and Ryan Babbush for discussions on fermionic marginal constraints. Furthermore, we thank Christian Gogolin and Maximilian Scheurer for input on shadow estimation. We thank Eugene DePrince III and Brecht Verstichel for discussions about the v2rdm method.

- 
- [1] D. S. Abrams and S. Lloyd, Simulation of many-body fermi systems on a universal quantum computer, *Physical Review Letters* **79**, 2586–2589 (1997).
  - [2] A. Aspuru-Guzik, A. D. Dutoi, P. J. Love, and M. Head-Gordon, Simulated quantum computation of molecular energies, *Science* **309**, 1704–1707 (2005).
  - [3] Y. Cao, J. Romero, J. P. Olson, M. Degroote, P. D. Johnson, M. Kieferová, I. D. Kivlichan, T. Menke, B. Peropadre, N. P. D. Sawaya, S. Sim, L. Veis, and A. Aspuru-Guzik, Quantum chemistry in the age of quantum computing, *Chemical Reviews* **119**, 10856–10915 (2019).
  - [4] S. McArdle, S. Endo, A. Aspuru-Guzik, S. C. Benjamin, and X. Yuan, Quantum computational chemistry, *Reviews of Modern Physics* **92**, 10.1103/revmodphys.92.015003 (2020).
  - [5] J. Preskill, Quantum computing in the nisq era and beyond, *Quantum* **2**, 79 (2018).
  - [6] W. J. Huggins, B. A. O’Gorman, N. C. Rubin, D. R. Reichman, R. Babbush, and J. Lee, Unbiasing fermionic quantum monte carlo with a quantum computer, *Nature* **603**, 416–420 (2022).
  - [7] M. Scheurer, G.-L. R. Anselmetti, O. Oumarou, C. Gogolin, and N. C. Rubin, Tailored and externally corrected coupled cluster with quantum inputs, *Journal of Chemical Theory and Computation* **20**, 5068 (2024).
  - [8] H.-Y. Huang, R. Kueng, and J. Preskill, Predicting many properties of a quantum system from very few measurements, *Nature Physics* **16**, 1050–1057 (2020).
  - [9] A. Zhao, N. C. Rubin, and A. Miyake, Fermionic partial tomography via classical shadows, *CoRR* (2020), [arXiv:2010.16094v1](https://arxiv.org/abs/2010.16094v1) [quant-ph].
  - [10] K. Wan, M. Berta, and E. T. Campbell, Randomized quantum algorithm for statistical phase estimation, *Physical Review Letters* **129**, 10.1103/physrevlett.129.030503 (2022).
  - [11] G. H. Low, Classical shadows of fermions with particle number symmetry, *CoRR* (2022), [arXiv:2208.08964](https://arxiv.org/abs/2208.08964) [quant-ph].
  - [12] H.-Y. Huang, M. Broughton, J. Cotler, S. Chen, J. Li, M. Mohseni, H. Neven, R. Babbush, R. Kueng, J. Preskill, and J. R. McClean, Quantum advantage in learning from experiments, *Science* **376**, 1182–1186 (2022).
  - [13] N. C. Rubin, R. Babbush, and J. McClean, Application of fermionic marginal constraints to hybrid quantum algorithms, *New Journal of Physics* **20**, 053020 (2018).
  - [14] F. Arute, K. Arya, R. Babbush, D. Bacon, J. C. Bardin, R. Barends, S. Boixo, M. Broughton, B. B. Buckley, D. A. Buell, B. Burkett, N. Bushnell, Y. Chen, Z. Chen, B. Chiaro, R. Collins, W. Courtney, S. Demura, A. Dunsworth, E. Farhi, A. Fowler, B. Foxen, C. Gidney, M. Giustina, R. Graff, S. Habegger, M. P. Harrigan, A. Ho, S. Hong, T. Huang, W. J. Huggins, L. Ioffe, S. V. Isakov, E. Jeffrey, Z. Jiang, C. Jones, D. Kafri, K. Kechedzhi, J. Kelly, S. Kim, P. V. Klimov, A. Korotkov, F. Kostritsa, D. Landhuis, P. Laptev, M. Lindmark, E. Lucero, O. Martin, J. M. Martinis, J. R. McClean, M. McEwen, A. Megrant, X. Mi, M. Mohseni, W. Mruczkiewicz, J. Mutus, O. Naaman, M. Neeley, C. Neill, H. Neven, M. Y. Niu, T. E. O’Brien, E. Ostby, A. Petukhov, H. Putterman, C. Quintana, P. Roushan, N. C. Rubin, D. Sank, K. J. Satzinger, V. Smelyanskiy, D. Strain, K. J. Sung, M. Szalay, T. Y. Takeshita, A. Vainsencher, T. White, N. Wiebe, Z. J. Yao, P. Yeh, and A. Zalcman, Hartree-fock on a superconducting qubit quantum computer, *Science* **369**, 1084–1089 (2020).
  - [15] I. Avdic and D. A. Mazziotti, Fewer measurements from shadow tomography with  $n$ -representability conditions, *Phys. Rev. Lett.* **132**, 220802 (2024).

- [16] A. Eugene DePrince III, Variational determination of the two-electron reduced density matrix: A tutorial review, *WIREs Computational Molecular Science* **14**, e1702 (2024).
- [17] B. Verstichel, H. van Aggelen, D. Van Neck, P. W. Ayers, and P. Bultinck, Variational density matrix optimization using semidefinite programming, *Computer Physics Communications* **182**, 2025 (2011), computer Physics Communications Special Edition for Conference on Computational Physics Trondheim, Norway, June 23-26, 2010.
- [18] S. Simon, R. Santagati, M. Degroote, N. Moll, M. Streif, and N. Wiebe, Improved precision scaling for simulating coupled quantum-classical dynamics, *PRX Quantum* **5**, 010343 (2024).
- [19] S. Simon, M. Degroote, N. Moll, R. Santagati, M. Streif, and N. Wiebe, **Amplified amplitude estimation: Exploiting prior knowledge to improve estimates of expectation values** (2024).
- [20] R. Santagati, A. Aspuru-Guzik, R. Babbush, M. Degroote, L. González, E. Kyoseva, N. Moll, M. Oppel, R. M. Parrish, N. C. Rubin, M. Streif, C. S. Tautermann, H. Weiss, N. Wiebe, and C. Utschig-Utschig, Drug design on quantum computers, *Nature Physics* , 1 (2024).
- [21] T. E. O’Brien, M. Streif, N. C. Rubin, R. Santagati, Y. Su, W. J. Huggins, J. J. Goings, N. Moll, E. Kyoseva, M. Degroote, C. S. Tautermann, J. Lee, D. W. Berry, N. Wiebe, and R. Babbush, Efficient quantum computation of molecular forces and other energy gradients, *Physical Review Research* **4**, 10.1103/physrevresearch.4.043210 (2022).
- [22] M. Steudtner, S. Morley-Short, W. Pol, S. Sim, C. L. Cortes, M. Loipersberger, R. M. Parrish, M. Degroote, N. Moll, R. Santagati, and M. Streif, Fault-tolerant quantum computation of molecular observables, *Quantum* **7**, 1164 (2023).
- [23] S. Aaronson, Shadow tomography of quantum states, *SIAM Journal on Computing* **49**, STOC18 (2020).
- [24] P.-O. Löwdin, Quantum theory of many-particle systems. i. physical interpretations by means of density matrices, natural spin-orbitals, and convergence problems in the method of configurational interaction, *Physical Review* **97**, 1474–1489 (1955).
- [25] J. E. Mayer, Electron correlation, *Physical Review* **100**, 1579–1586 (1955).
- [26] A. E. D. III., “libSDP: a library of semidefinite programming solvers” (2021).
- [27] J. Povh, F. Rendl, and A. Wiegele, A boundary point method to solve semidefinite programs, *Computing* **78**, 277–286 (2006).
- [28] J. Malick, J. Povh, F. Rendl, and A. Wiegele, Regularization methods for semidefinite programming, *SIAM Journal on Optimization* **20**, 336–356 (2009).
- [29] D. A. Mazziotti, Large-scale semidefinite programming for many-electron quantum mechanics, *Physical Review Letters* **106**, 10.1103/physrevlett.106.083001 (2011).
- [30] D. A. Mazziotti, Realization of quantum chemistry without wave functions through first-order semidefinite programming, *Physical Review Letters* **93**, 10.1103/physrevlett.93.213001 (2004).
- [31] M. Kiser, A. Schroeder, G.-L. R. Anselmetti, C. Kumar, N. Moll, M. Streif, and D. Vodola, Classical and quantum cost of measurement strategies for quantum-enhanced auxiliary field quantum monte carlo, *New Journal of Physics* **26**, 033022 (2024).
- [32] J. R. McClean, N. C. Rubin, K. J. Sung, I. D. Kivlichan, X. Bonet-Monroig, Y. Cao, C. Dai, E. S. Fried, C. Gidney, B. Gimby, P. Gokhale, T. Häner, T. Hardikar, V. Havlíček, O. Higgott, C. Huang, J. Izaac, Z. Jiang, X. Liu, S. McArdle, M. Neeley, T. O’Brien, B. O’Gorman, I. Ozfidan, M. D. Radin, J. Romero, N. P. D. Sawaya, B. Senjean, K. Setia, S. Sim, D. S. Steiger, M. Steudtner, Q. Sun, W. Sun, D. Wang, F. Zhang, and R. Babbush, Openfermion: the electronic structure package for quantum computers, *Quantum Science and Technology* **5**, 034014 (2020).
- [33] V. von Burg, G. H. Low, T. Häner, D. S. Steiger, M. Reiher, M. Roetteler, and M. Troyer, Quantum computing enhanced computational catalysis, *Physical Review Research* **3**, 10.1103/physrevresearch.3.033055 (2021).
- [34] O. Oumarou, M. Scheurer, R. M. Parrish, E. G. Hohenstein, and C. Gogolin, Accelerating Quantum Computations of Chemistry Through Regularized Compressed Double Factorization, *Quantum* **8**, 1371 (2024).
- [35] J. Lee, D. W. Berry, C. Gidney, W. J. Huggins, J. R. McClean, N. Wiebe, and R. Babbush, Even more efficient quantum computations of chemistry through tensor hypercontraction, *PRX Quantum* **2**, 10.1103/prxquantum.2.030305 (2021).
- [36] R. King, D. Gosset, R. Kothari, and R. Babbush, Triply efficient shadow tomography, *arXiv e-prints* , arXiv:2404.19211 (2024).
- [37] A. Zhao and A. Miyake, Group-theoretic error mitigation enabled by classical shadows and symmetries, *CoRR* (2023), arXiv:2310.03071 [quant-ph].

## Appendix A: Spin restricted v2rdm

As we work in a spin-adapted setting, one can further find a sub-block structure of the positive-semidefinite matrices. We decompose the 1-particle density matrix  ${}^1\mathbf{D}^{pq} = \langle \psi | a_p^\dagger a_q | \psi \rangle$  and its derivate  ${}^1\mathbf{Q}^{pq} = \langle \psi | a_p a_q^\dagger | \psi \rangle$  into spin-blocks in the following way, as discussed in further depth in [13]

$${}^1\mathbf{D} = \begin{pmatrix} {}^1\mathbf{D}_\alpha & 0 \\ 0 & {}^1\mathbf{D}_\beta \end{pmatrix} \quad (\text{A1})$$

and  $Q$

$${}^1\mathbf{Q} = \begin{pmatrix} {}^1\mathbf{Q}_\alpha & 0 \\ 0 & {}^1\mathbf{Q}_\beta \end{pmatrix} \quad (\text{A2})$$

The two particle conditions of  ${}^2\mathbf{D}^{pqrs} = \langle \psi | a_p^\dagger a_q^\dagger a_s a_r | \psi \rangle$  and derived quantities  ${}^2\mathbf{Q}^{pqrs} = \langle \psi | a_p^\dagger a_q a_s^\dagger a_r | \psi \rangle$  and  ${}^2\mathbf{Q}^{pqrs} = \langle \psi | a_p a_q a_s^\dagger a_r^\dagger | \psi \rangle$  can also further be block diagonalized into spin sectors. For compactness sake, we leave out the upper indices on the diagonal  ${}^2\mathbf{D}_{\alpha\alpha} \equiv {}^2\mathbf{D}_{\alpha\alpha}^{\alpha\alpha}$  and get four spin-blocks for the 2-RDM

$${}^2\mathbf{D} = \begin{pmatrix} {}^2\mathbf{D}_{\alpha\alpha} & 0 & 0 & 0 \\ 0 & {}^1\mathbf{D}_{\beta\beta} & 0 & 0 \\ 0 & 0 & {}^2\mathbf{D}_{\alpha\beta} & 0 \\ 0 & 0 & 0 & {}^2\mathbf{D}_{\beta\alpha} \end{pmatrix} \quad (\text{A3})$$





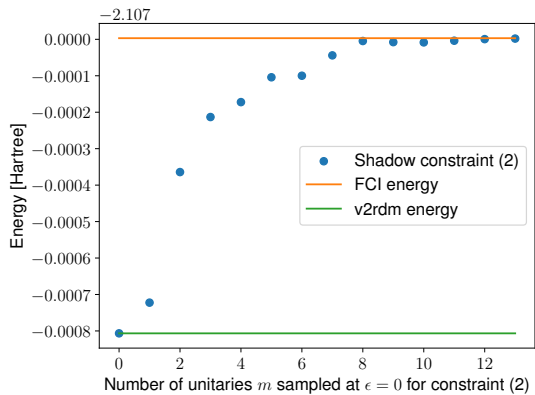


FIG. 3. Energy convergence for H2 for the optimisation under shadow constraint (2) in dependence of number of basis  $m$  used for additional constraints during optimisation.

H4 in STO-3G the energy convergence in Fig 3 in dependence of the number of basis sampled  $m$ , also reaching exact agreement at  $m = 12$  basis used for the additional constraints during optimisation at infinite precision, corresponding to taking an infinite number of shots at each basis. So we deem our implementation of the shadow constraint comparable to the one studied in previous work.